# $u_{\mu} \rightarrow \nu_{\tau}$ Appearance in $\mu$ BooNE REU Program at Columbia University - Nevis Labs

## Sarah Vickers<sup>1</sup>

<sup>1</sup>University of North Carolina at Chapel Hill

August 4, 2023

#### Abstract

The MicroBooNE collaboration and greater Short Baseline Neutrino Program at Fermilab are part of the current generation of neutrino experiments probing for new physics beyond the Standard Model. The primary goal of SBN is searching for the possibility of light sterile neutrinos through  $\nu_{\mu} \to \nu_{e}$  oscillations and  $\nu_{\mu}$  disappearance. This analysis focuses on the possibility of sterile neutrino detection through the appearance of  $\nu_{\tau}$  via  $\nu_{\mu} \to \nu_{\tau}$  oscillations. As the first attempt to do so with MicroBooNE data, presented here are the initial steps towards establishing the first sensitivity to  $\nu_{\mu} \to \nu_{\tau}$  oscillation in MicroBooNE. Focusing mostly on MC truth-level information, an in-depth study of the kinematics of  $\nu_{\tau}$ CC interactions and background  $\nu_{e}$ CC interactions was conducted. Tools for optimizing background rejection and signal selection were developed for further testing with reconstruction information. Preliminary study indicates that the low statistics available in the high energy region required for tau production would make detection of any significant  $\nu_{\mu} \to \nu_{\tau}$  signal improbable.



# Contents

1	Introduction	3	
	1.1 The MicroBooNE Experiment	3	
	1.2 LArTPCs	4	
	1.3 Booster Neutrino Beam	4	
2	$ u_{\mu} \rightarrow \nu_{\tau} $ Oscillation	5	
	2.1 Interactions & Decay Schemes	6	
	2.2 $\nu_{\tau}$ CC Kinematics	6	
	2.3 Kinematic Variables		
3	Truth-Level Analysis	8	
	3.1 GENIE	8	
	3.2 Event Pre-selection	9	
	3.3 Kinematic Selections	11	
	3.4 POT Normalization & Significance	11	
	3.5 Correlation	13	
	3.5.1 2D Selections	13	
4	Reconstruction Analysis 14		
5	Conclusion & Next Steps	16	
6	Acknowledgements		
7	Appendix	19	

## Contact me at:

Phone #: (859) 749-8597

University Affiliated Email (effective until January 2024): svickers@email.unc.edu

Non-Affiliated Email: vickerselsarah@gmail.com

# 1 Introduction

Since the proposal of the elusive particle by Wolfgang Pauli nearly a century ago, the neutrino has been at the heart of many long-standing questions about the standard model of particle physics, astrophysical phenomena and the beginning of our universe. One of the remaining mysteries of the neutrino is that of the extremely small neutrino mass, with several experiments around the world working to improve the known limits of neutrino mass and determine the ranking of masses between the three flavors. The MiniBooNE experiment was one of these, a liquid scintillator detector seeking to confirm or deny the results from the Los Alamos Liquid Scintillator Neutrino Detector (LSND), which indicated an anomalous mass-squared difference of  $\sim 1~{\rm eV^2}$  [3]. The results of MiniBooNE showed an excess of low-energy neutrino events to  $> 4\sigma$ , contributing to a list of experimental anomalies in neutrino physics [2]. These anomalies motivate the theory of a fourth type of neutrino, the sterile neutrino, in addition to the three flavors currently in the SM, which does not interact via the weak force. While not directly detectable through weak force interactions, sterile neutrinos could have a hand in observable short-baseline neutrino oscillation signatures between the other three flavors. Confirmation of the sterile neutrino would be proof of physics beyond the Standard Model, of great interest to the physics community.

The MiniBooNE low-energy excess could be explained by single electron or single photon interactions, which MiniBooNE did not have the capability to distinguish. MicroBooNE, as a LArTPC experiment, has the capability to distinguish between the two types of event, investigating the source of the MiniBooNE low energy excess and continuing to search for signs of the sterile neutrino.

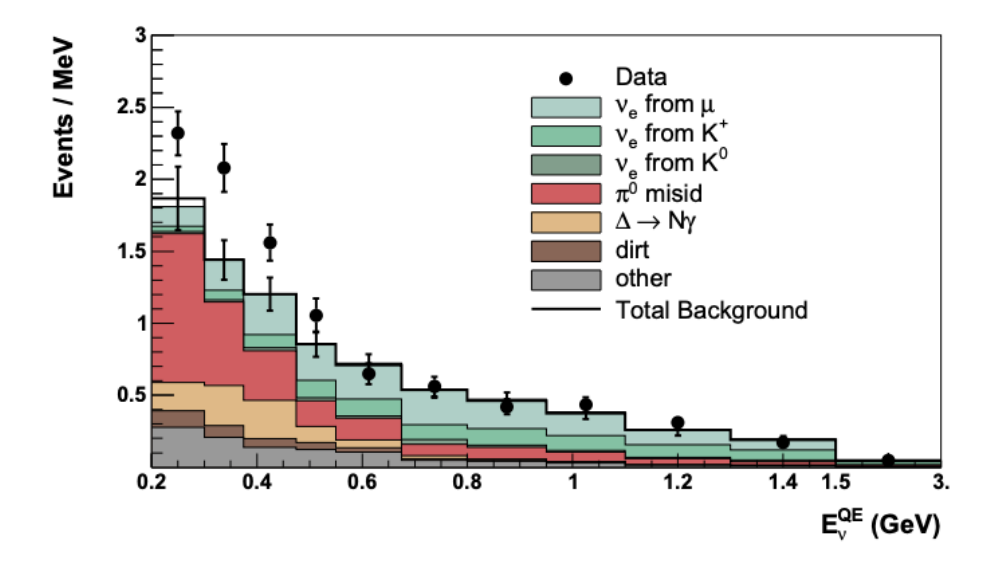


Figure 1: MiniBooNE low-energy excess [2].

# 1.1 The MicroBooNE Experiment

MicroBooNE is a 170-ton liquid argon time projection chamber (LArTPC) placed on the Booster Neutrino Beamline at Fermilab in Batavia, Illinois. At 468 meters down-beam, it is the mid-distance detector of the Short Baseline Neutrino (SBN) program, further consisting of ICARUS (far detector at 600 meters) and the Short Baseline Near Detector (SBND, at 110 meters). MicroBooNE was

the first large-scale LArTPC to collect high statistics data on neutrino interactions, completing five runs from 2015-2020. In addition to its own physics goals, this was a major step in development for the future of kiloton-scale liquid argon detectors such as DUNE. As stated, the primary goal of MicroBooNE and the greater SBN program is to search for light sterile neutrinos in the  $\Delta m^2 \sim 1$  eV<sup>2</sup> range via  $\nu\mu \to \nu_e$  oscillations [1].



Figure 2: The three detectors which make up the SBN Program [7].

#### 1.2 LArTPCs

Liquid argon time projection chambers are the present and future of neutrino research, with MicroBooNE being the largest successful demonstration of the technology's usefulness as a neutrino detector. Cold liquid argon acts as the nucleon target for neutrino interactions, an ideal candidate due to its density and cost efficiency. A cathode plane on one wall of the detector is held at high voltage, and any ionized particles in the chamber drift across the volume to the opposite side, where three wire planes catch and record the drift current. Each of the wire planes are held at 60 degree offset to one another, allowing spacial reconstruction in the y-z plane. Additional timing information from PMT flashes and wire-hit timing provides the remaining reconstruction in the x-component [5].

#### 1.3 Booster Neutrino Beam

The Fermilab Booster Neutrino Beam is generated by accelerating 8 GeV protons into a Beryllium target in 5 Hz pulses with  $5 \cdot 10^{12}$  protons per pulse. Runs 1-3 of MicroBooNE had a total of  $6.8 \cdot 10^{20}$ 

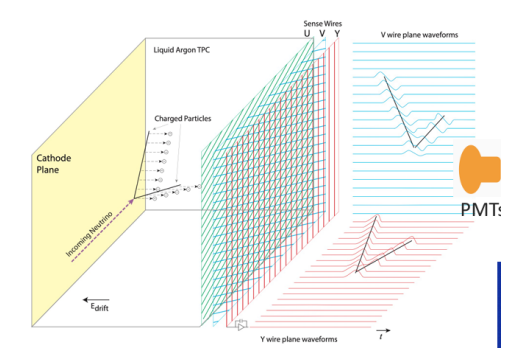


Figure 3: LArTPC wire plane diagram for MicroBooNE- events are identified and reconstructed by PMT array and three wire planes to catch ionized particles [6].

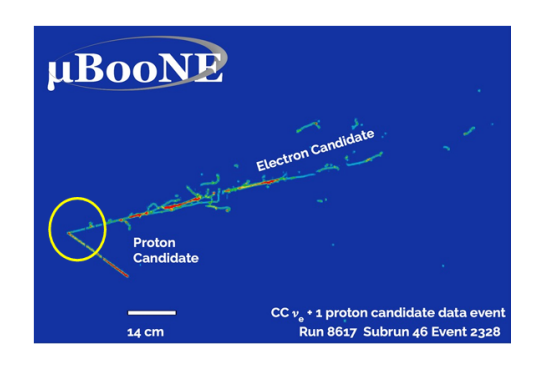


Figure 4: A reconstructed  $\nu_e CC$  event.

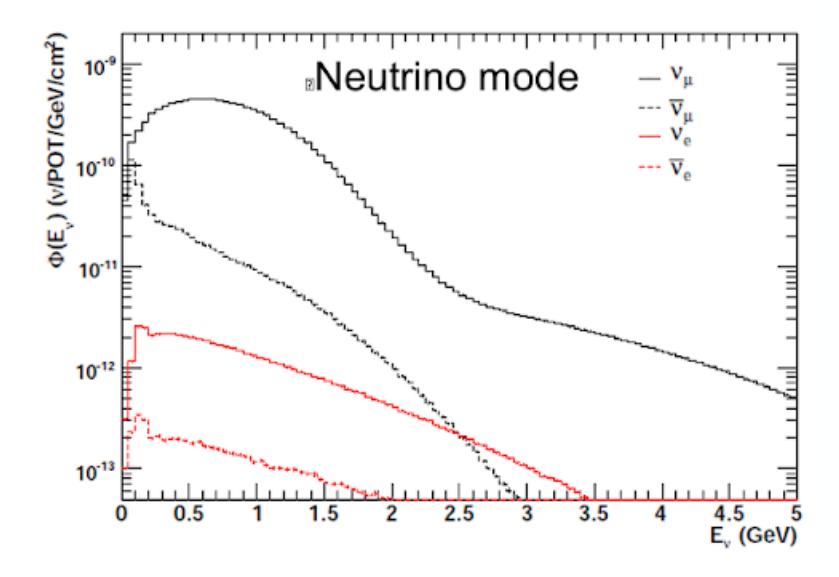
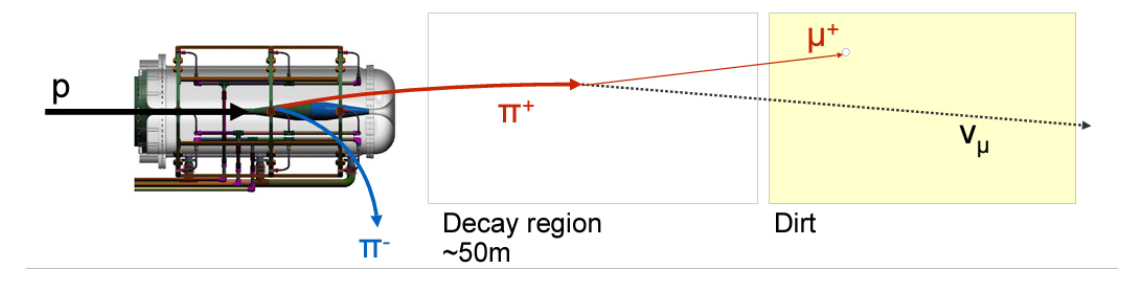


Figure 5: BNB neutrino mode flux as a function of neutrino energy [1].

protons-on-target (POT), and over all five runs accumulated a POT of  $1.32 \cdot 10^{21}$ . This generates a beam of negative and positively charged pions, wherein the  $\Pi^+$ s decay into muons and  $\nu_{\mu}$ s, giving a primarily  $\nu_{\mu}$  flux through the detector. The neutrino mode flux can be seen in Fig. 5. The peak  $\nu_{\mu}$  energy is calibrated to the maximum oscillation probability for a  $\Delta m^2$  in the 1 eV<sup>2</sup> range.

# 2 $\nu_{\mu} \rightarrow \nu_{\tau}$ Oscillation

MicroBooNE initially searched for evidence of light sterile neutrinos in the form of  $\nu_{\mu} \rightarrow \nu_{e}$  oscillations. The first constraints on this process were published in late 2022, having not found any indication of oscillations (although at a low sensitivity) [4]. Turning to other possible oscillation candidates, this analysis focuses on  $\nu_{\mu} \rightarrow \nu_{\tau}$  oscillations, unstudied thus far using MicroBooNE data. This study continues the beginning of an investigation into the MicroBooNE and greater SBN program sensitivity to  $\nu_{\mu} \rightarrow \nu_{\tau}$  oscillation. Previous sensitivity calculations for this oscillation have been carried out for the NOMAD, CHORUS and OPERA experiments, as well as preliminary analysis for DUNE at long-baseline.



**Figure 6:** Creation of the  $\nu_{\mu}$  Booster Neutrino Beam.

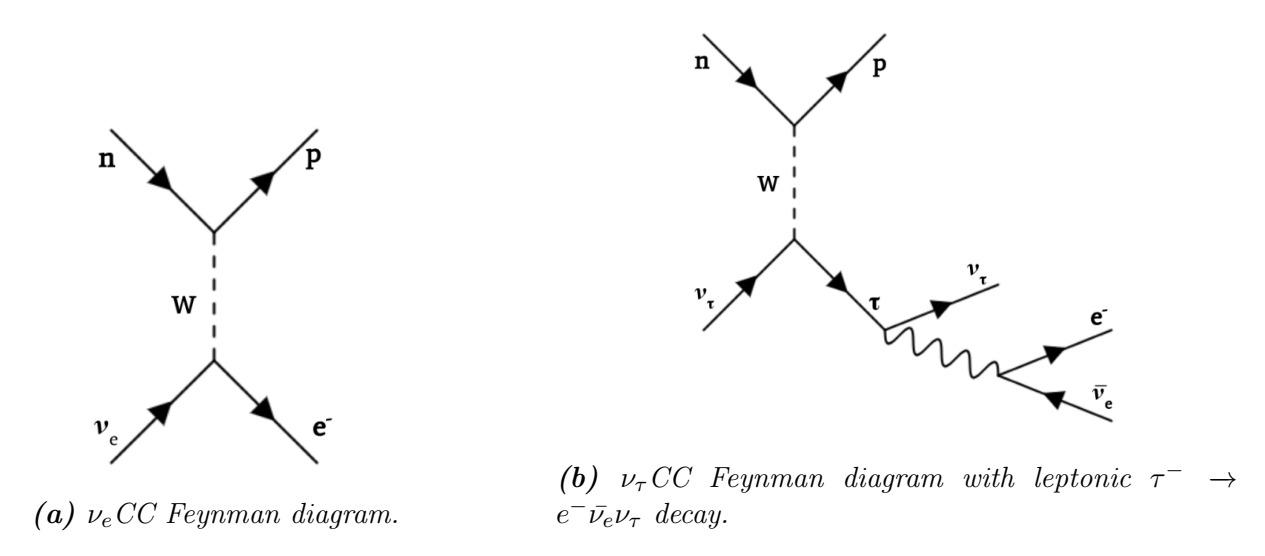


Figure 7: Background (left) vs. Signal (right)

## 2.1 Interactions & Decay Schemes

Neutrino-nucleon interactions can occur through neutral current (NC) interactions which involve the exchange of W<sup>+/-</sup> boson, or charged current (CC) interactions which involve the exchange of a Z boson. NC interactions are elastic, where the nucleon is not changed by the neutrino, and are therefore of little interest to this analysis. CC interactions are quasi-elastic, resulting in the emission of a changed nucleon and the appropriate lepton. While NC interactions may occur at any incident neutrino energy, CC interactions transfer mass to the final state lepton - requiring a threshold neutrino energy. As the heaviest lepton, the  $\nu_{\tau}$ CC interaction has the highest threshold energy of the three flavors at  $\sim 3.5$  GeV. As seen in Fig. 5, the  $\nu_{\mu}$  flux is comparatively low in the high energy region > 3.5 GeV, a significant consideration that results in few  $\nu_{\tau}$ CC interactions for the total POT of MicroBooNE. For comparison, the  $\nu_{e}$ CC threshold in MicroBooNE is as low as 60 MeV.

Another complication comes in the lifetime of the outgoing leptons generated by these interactions. In  $\nu_e$ CC and  $\nu_\mu$ CC interactions, the resulting electron or muon as well as the outgoing proton will leave a track in the LArTPC that allows direct reconstruction of the final state particles. The tau created by the  $\nu_\tau$ CC interaction does not live long enough for its track to be picked up by the wire planes, leaving behind leptonic or hadronic decay products which do have identifiable tracks. Restricting to leptonic tau decay, the two possible outcomes are that of  $\tau^- \to \mu^- \bar{\nu}_\mu \nu_\tau$  and  $\tau^- \to e^- \bar{\nu}_e \nu_\tau$  with branching ratios of 17.39% and 17.82% respectively [8]. A full table of the tau decay schemes for hadronic and leptonic processes can be seen in Table 1 in the Appendix. As the beam flux is majority  $\nu_\mu$ , the muon decay scheme is abandoned and we are left with the remaining electron decay scheme as our signal events. The obvious background to this process are the  $\nu_e$ CC interactions that also provide a final state electron and proton. The upside here is that the  $\nu_e$  content of the beam flux is quite small, providing a relatively low background when focusing only on tau events which generate a final state electron.

# 2.2 $\nu_{\tau}$ CC Kinematics

Where these two signals differ is in the kinematics of the final state particles. The  $\nu_{\tau}$ CC interaction and subsequent decay release an additional neutrino and antineutrino that carry away a portion of the

momentum and energy of the process. This is evident in the transverse momentum of the outgoing charged particles. A reconstructed  $\nu_e$ CC event with visible electron and proton tracks should have a total transverse momentum close to zero, whereas a  $\nu_{\tau}$  event with similar reconstructed events would be missing the transverse momentum carried away by the neutrino and antineutrino. To accurately simulate this, at least two models must be included, one for the neutrino-nucleon scattering itself and one for the movement of the nuclei (its Fermi momentum). GENIE accounts for both of these models, resulting in a non-zero (but smaller than  $\nu_{\tau}$ )  $\nu_e$ CC total transverse momentum.

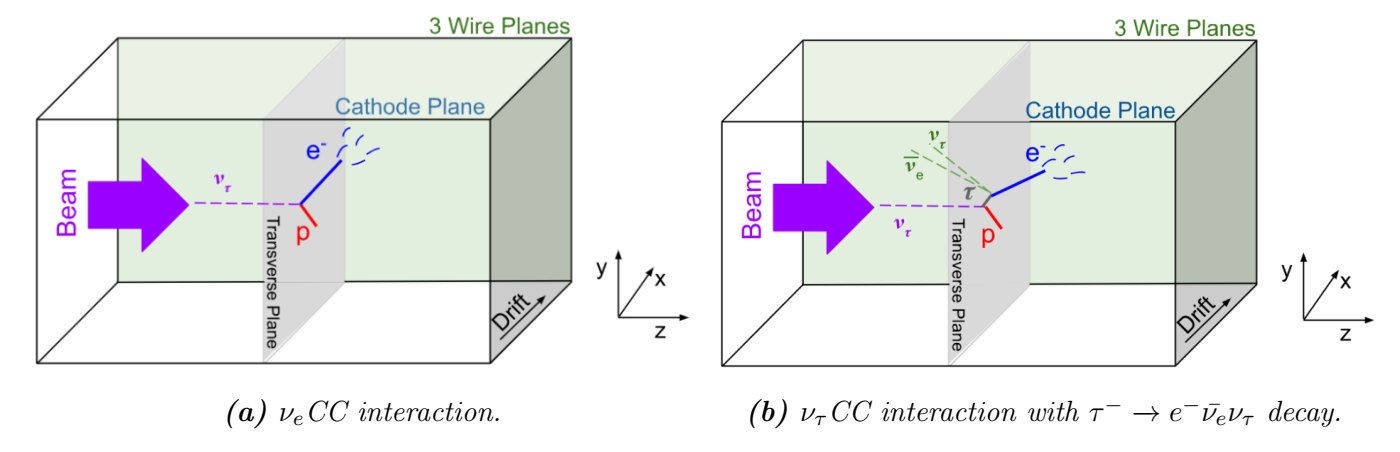


Figure 8: Background (left) vs. Signal (right)

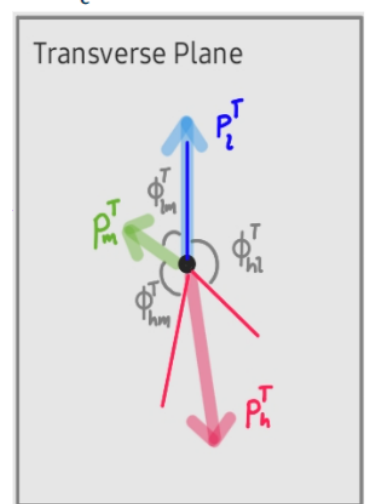
#### 2.3 Kinematic Variables

This analysis is largely unconcerned with the on-beam (z) directionality of the events, focusing on the transverse (perpendicular to the beam) plane. This is because nearly all of the neutrino momentum is along the z-direction, so the lack of momentum in the transverse plane must be conserved.

The seven key variables used in the MC-truth analysis are as follows:

- $\bullet$  p<sup>T</sup> The total transverse momentum of the interaction, using the momentum of the outgoing leptons and hadrons of the event.
  - The primary lepton of concern is always an electron, for both interactions. Different analysis schemes call for taking into account only the maximum energy proton, the total proton momentum, or event the collection of all charged particles which leave a track ( protons, pions, kaons, etc.).
- $\mathbf{p}_p^T$  The transverse momentum of the outgoing hadron(s), such as protons (calculated using the momentum of all protons which meet the pre-selection KE threshold more on this in section 3.2).
- $\bullet~\mathbf{p}_e^T$  The transverse momentum of the outgoing lepton (electron).
- KE<sub>lep</sub> Kinetic Energy of the outgoing lepton (electron).
- $\phi_{lm}$  Transverse angle between the outgoing lepton  $\mathbf{p}_l^T$  and the missing transverse momentum  $\mathbf{p}^T$ .

## ν<sub>c</sub>CC Interaction



## ν<sub>c</sub>CC Interaction

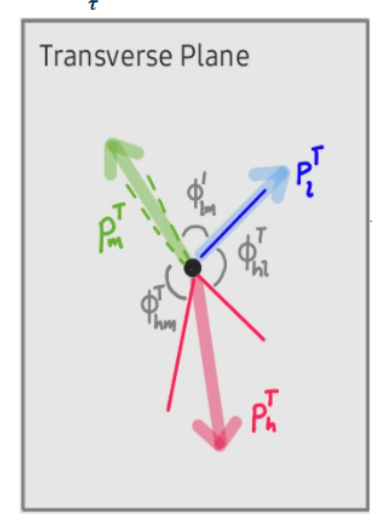


Figure 9: Background (left) vs. Signal (right)

- $\phi_{lh}$  Transverse angle between the outgoing lepton  $\mathbf{p}_l^T$  and the outgoing hadronic  $\mathbf{p}_h^T$ .
- $\phi_{hm}$  Transverse angle between the outgoing hadronic  $\mathbf{p}_h^T$  and the missing transverse momentum  $\mathbf{p}^T$ .

All of these variables tell us important information about the events we are looking at, and helped in developing the selections. See section 3.3 to see the distributions of each variable.

One of the first determinations of the study was made here, in choosing how to calculate the proton transverse momentum. There is only one electron per event, but there can be multiple final state protons ejected from the nucleus due to nuclear effects. In the following plots, we compare the usage of the total proton momentum (the summed momentum of all final state protons) and taking only the momentum of the proton with the maximum kinetic energy. From the distributions it is evident that there is better  $p^T$  separation between signal and background when the total proton momentum is used, so going forward all  $p^T$  calculations take into account all protons which meet the kinetic energy threshold for the particular pre-selection.

# 3 Truth-Level Analysis

## 3.1 GENIE

The Monte Carlo data analyzed here was obtained using the GENIE (Generates Events for Neutrino Interaction Experiments) neutrino generator. Using the intrinsic  $\nu_e$  flux from BNB, a POT of  $2.56 \cdot 10^{22}$  was needed to generate 19,280 simulated  $\nu_e$ CC events. Assuming  $100\% \nu_\mu \to \nu_\tau$  oscillation, a POT of  $1.51 \cdot 10^{23}$  generated 19,120  $\nu_\tau$ CC events. For the  $\nu\tau$  events, each  $\tau$  decay scheme is present with respect to its branching ratio (see Table 1), so the number of true  $\nu_\tau$  with  $\tau^- \to e^- \bar{\nu}_e \nu_\tau$  was reduced to 3,363. The POT required to acquire this many events is much higher than the full run 1-5 POT for MicroBooNE, and requires normalization later on in the analysis.

The MC-truth information was then fed through the Pandora pattern recognition software for simulated reconstruction, which is used by the MicroBooNE collaboration. This gives the reconstruc-

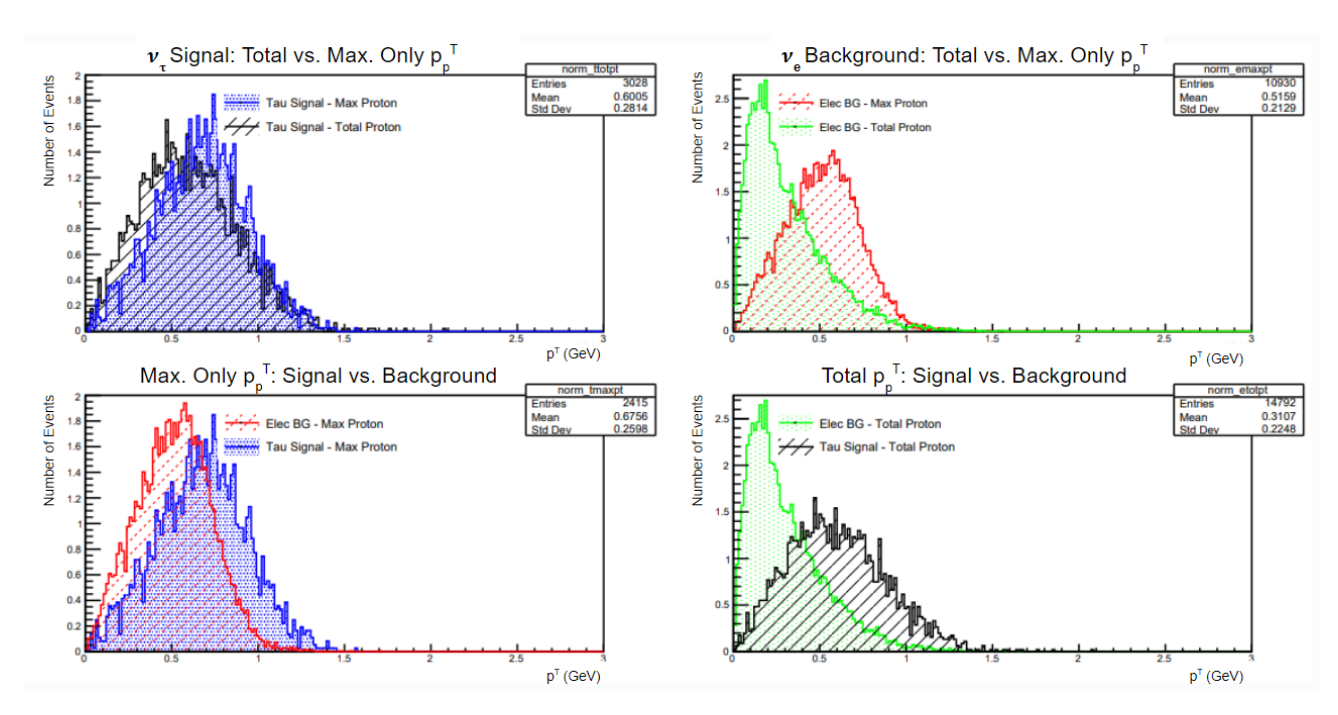


Figure 10:  $p^T$  distributions for two  $p_p^T$  considerations, with a 50 MeV proton kinetic energy threshold.

tion information, a much better representation of what true MicroBooNE data looks like, which is used in the last section of the analysis done here and will be used further in next steps for the project.

## 3.2 Event Pre-selection

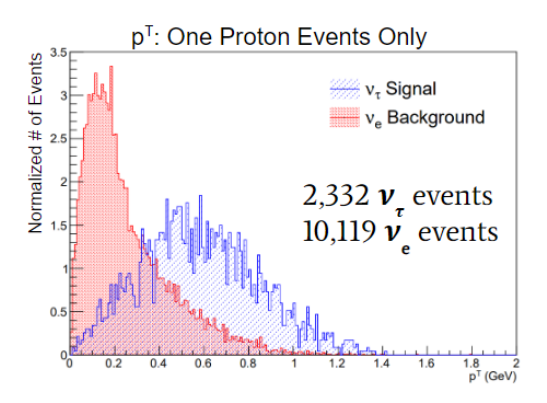
Given the MC-truth information, pre-selections must be made on the outgoing final state particles to select the events that we want to look at. The minimum a given event must have for it to be of use to this analysis is to be a true CC interaction, with an outgoing electron and at least one final state proton. For the  $\nu_{\tau}$  data, it was also required that the mother particle of the outgoing electron must be a tau.

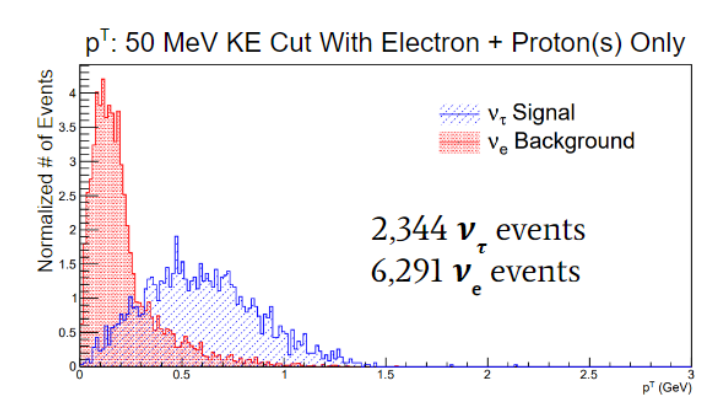
Once this base selection was applied, a variety of other event selection criteria were used on the remaining events. The two motivations for doing this were to either maximize separation between signal and background kinematic distributions or to improve the ratio of signal to background events. The various proton kinetic energy threshold are due to the ability of MicroBooNE to recreate proton tracks with small kinetic energies, where the threshold for reconstruction is  $\sim 30$  MeV and the threshold for good reconstruction with efficient particle identification is  $\sim 50$  MeV. All protons below 30 MeV are unlikely to be visible in true MicroBooNE data.

A list of the selection criteria studied can be seen below:

- Only taking into account the maximum energy proton (when calculating  $\mathbf{p}^T$ ,  $\mathbf{p}_h^T$  and other subsequent vars.).
  - With no proton KE minimum threshold
  - With a 30 MeV proton KE minimum threshold
  - With a 50 MeV proton KE minimum threshold
- Taking into account the sum of all final state protons
  - With no proton KE minimum threshold

- With a 30 MeV proton KE minimum threshold
- With a 50 MeV proton KE minimum threshold
- Filtering out all events that have any charged final state particles other than protons and electrons.
  - With no proton KE minimum threshold
  - With a 30 MeV proton KE minimum threshold
  - With a 50 MeV proton KE minimum threshold
- Filtering out all events that have more than one final state proton.
  - With no proton KE minimum threshold
  - With a 40 MeV proton KE minimum threshold
- Filtering to leave only events which only have one final state proton AND has no other final state charged particles.
  - With no proton KE minimum threshold





(a)  $p^T$  for one proton events only with no proton KE(b)  $p^T$  for events with no other charged particles in the threshold.

final state and a 50 MeV proton KE threshold.

Figure 11: Two  $p^T$  distributions.

Naturally, the optimal pre-selection criteria would keep as many signal events as possible while discarding as many background events as possible. Since the  $\nu_{\tau}$  events use up a lot of their energy in producing the heavy tau particle, there is less left over energy to produce other final state charged particles (the fill list of final state particles for the simulated  $\nu_{\tau}$ CC and  $\nu_{e}$ CC events, along with their kinetic energy distributions can be seen in the Appendix). Therefore, by filtering out any events which have outgoing particles other than the proton(s) and electron, we can greatly improve our ratio of signal to background events. For example, looking at only one proton events, before filtering out events with extra charged particles we have 2,332  $\nu_{\tau}$  events and 10,119  $\nu_{e}$  events. After filtering out events with extra charged particles, we have 1,836  $\nu_{\tau}$  events and 4,336  $\nu_{e}$  events. Similarly, when looking at events with any number of protons and a 50 MeV proton energy cutoff, before filtering out events with extra charged particles there are 3,028  $\nu_{\tau}$  events and 14,792  $\nu_{e}$  events, which is then reduced to 2,334  $\nu_{\tau}$  events and 6,291  $\nu_{e}$  events.

## 3.3 Kinematic Selections

As discussed, one of the main objectives in this analysis is to find the best kinematic separations between  $\nu_{\tau}$ CC and  $\nu_{e}$ CC interactions. The most basic filter gives all events which may be seen well in reconstruction, meaning any event with an electron (from the tau in the case of  $\nu_{\tau}$ ) and at least one proton with kinetic energy > 50 MeV. This is the most inclusive scheme which best reflects what we will see from MicroBooNE, and is therefore the metric against which the other pre-selections are measured. For the purposes of just looking at the kinematic differences, the signal and background histograms are normalized to the area under the curve (remember that there is a factor of 4-5 times more  $\nu_{e}$  events than  $\nu_{\tau}$  for this particular pre-selection).

# $v_{\tau} \, \text{Signal} \\ v_{e} \, \text{Background}$

## pT: Signal vs. Background

Figure 12:  $p^T$  with a 50 MeV proton kinetic energy threshold.

# 3.4 POT Normalization & Significance

To determine good cuts for the 1D selection, significance plots were created to maximize the significance of signal over background. Since the MC data has high enough statistics and is then normalized down to represent the true MicroBooNE POT, the standard method of calculating significance as signal over the square root of the background is viable, as opposed to other methods designed for low statistics measurements. For the significance calculations,  $x_0$  begins at the first bin and moves up a singular bin for each point, where  $x_1$  is always the last bin of the histogram. In essence, each point on the significance curve represents the signal significance if you were to count all events in the bins to the right of that point (for the  $\phi$  variables this was done opposite, calculating all events to the left of the point, as the background events tended to skew to the right for all three). In this way, it is possible to see where the cut should be made to have the highest  $\sigma$  of statistical significance, acting as a metric for making selections.

One of the true challenges of this analysis is the small number of viable  $\nu_{\tau}$ CC events. After POT normalization to the full run 1-5 POT of 1.32 ·10<sup>23</sup>, depending on the inclusion scheme there are 18-24 signal events assuming 100% oscillation. Giving a more realistic oscillation probability of 10%,

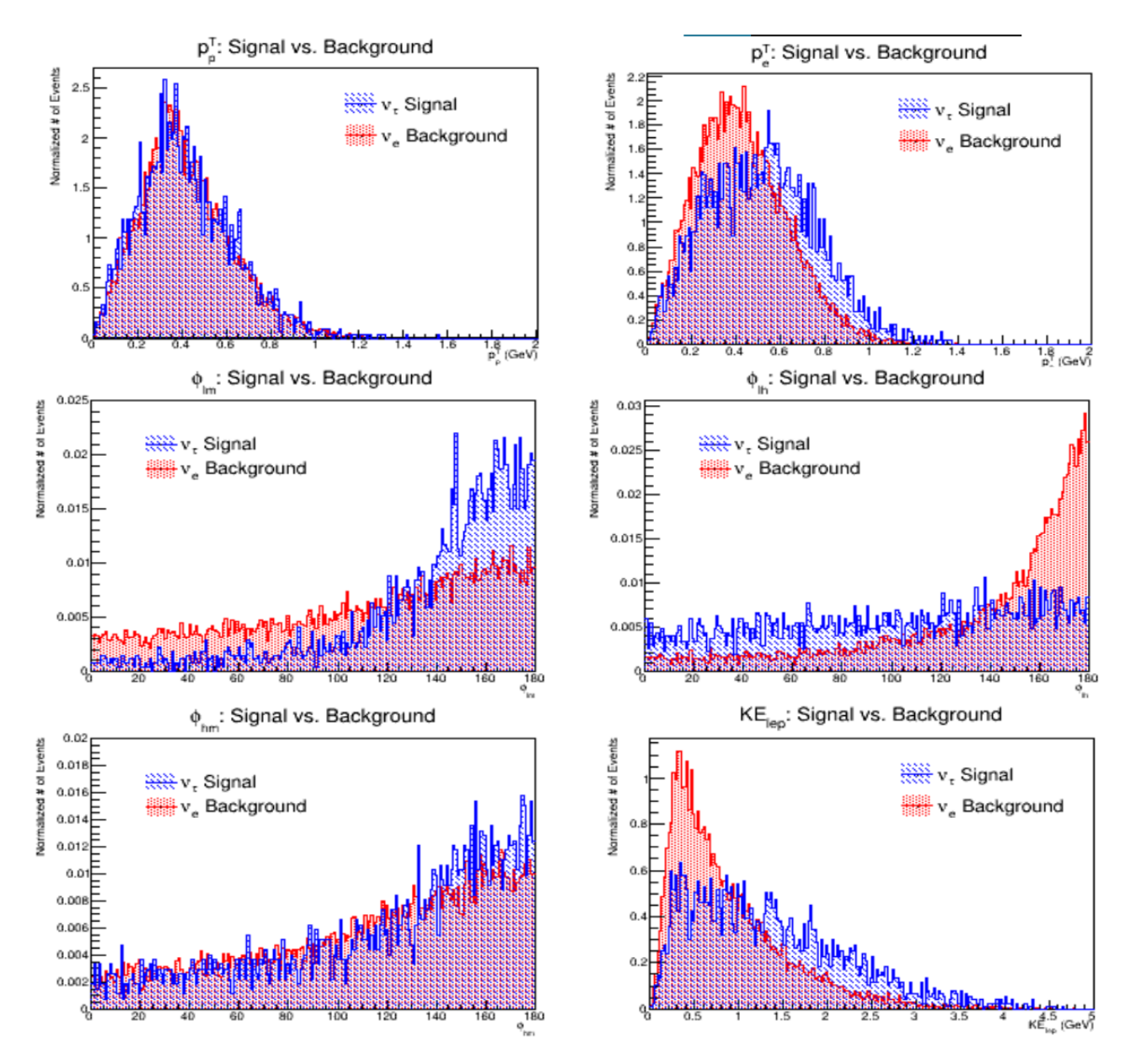


Figure 13:  $p_p^T$ ,  $p_e^T$ ,  $\phi_{lm}$ ,  $\phi_{lm}$ ,  $\phi_{hm}$  &  $KE_{lep}$  with a 50 MeV proton kinetic energy threshold.

this leaves us with 1-2 signal events over the entire MicroBooNE runtime. With this few events, it is virtually impossible to have any amount of statistical significance, even if you were able to achieve 100% background rejection. Restricting to only runs 1-3 data from MicroBooNE, all of these event counts are further reduced by a factor of  $\sim 2$ . The greater SBN program will of course have higher statistics than MicroBooNE alone, but again this would require an extraordinarily efficient background rejection algorithm for all three experiments.

$$S = \frac{\int_{x_0}^{x_1} Signal}{\sqrt{\int_{x_0}^{x_1} Background}} \tag{1}$$

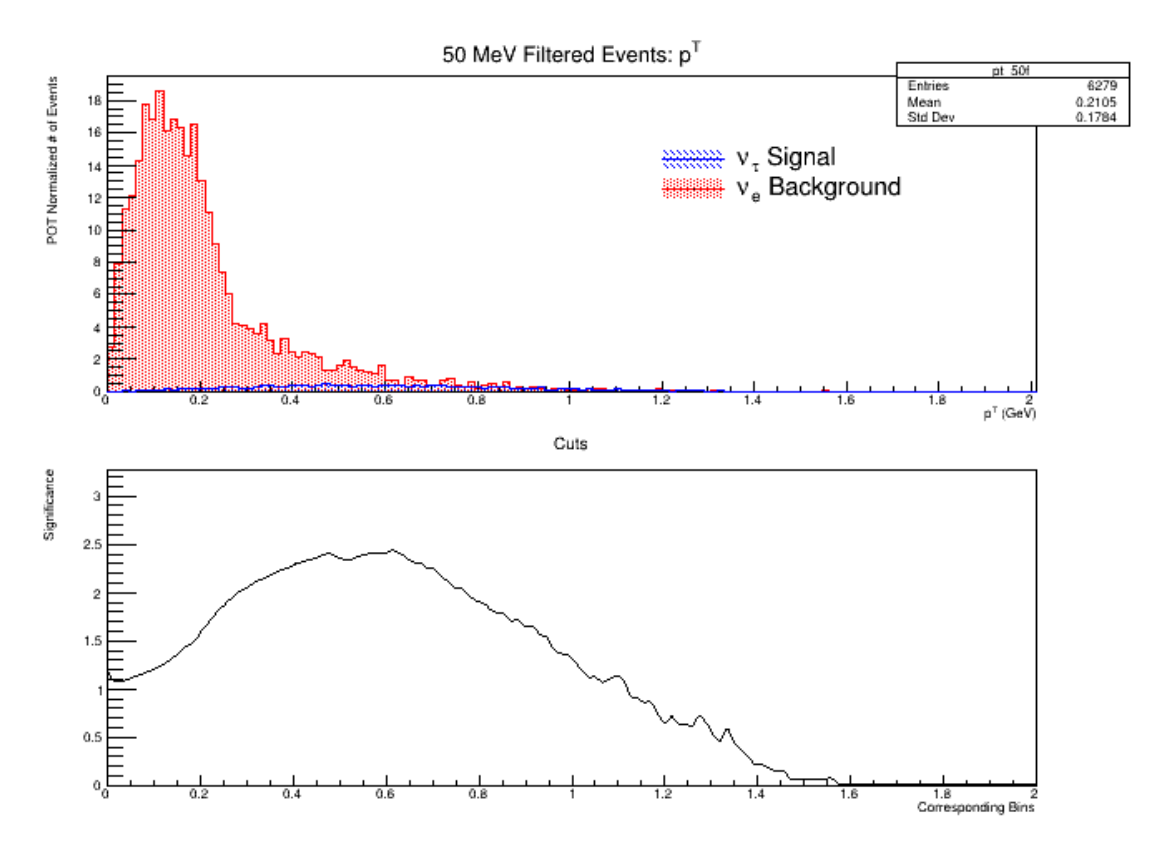


Figure 14: POT normalized  $p^T$  with corresponding significance plot - peak at  $\sim 0.45~GeV$ 

## 3.5 Correlation

To understand how these 1D distributions relate to one another, and where two dimensional differences are prominent, correlation matrices were made for two filtering schemes. The simple 50 MeV proton cutoff using the momentum of all protons, as well as the 50 MeV cutoff using the momentum of all protons, filtered to exclude all events with other charged particles. For the 50 MeV cutoff filter which does include events with other charged particles, three methods of calculating  $p^T$  were used: standard  $p^T$  taking into account only the electron and proton(s) momentum,  $p_c^T$  taking into account all charged particles' momentum, and  $p_{c+n}^T$  taking into account all particles' (neutral and charged) momentum (the effective Fermi momentum of the neutron).

From these plots we can determine some variables which are more or less correlated between signal and background, indicating where to look when making two-dimensional kinematic cuts. Some clear examples of this for the filtered events are seen in the strengthening of correlation between  $\phi_{hm}$  and  $\phi_{lm}$ , as well as between  $p_p^T$  and  $p_e^T$  when moving from  $nu_{tau}$  to  $\nu_e$  interactions.

#### 3.5.1 2D Selections

As  $p^T$  and  $\phi_{lh}$  had the highest significance and the most effective one dimensional cuts to get rid of background events, the next obvious step is to look at the correlation between the two variables and determine a viable two dimensional cut. The correlation matrices in Fig. 22 also show a large difference in the magnitude of correlation between signal and background for  $\phi_{hm}$  and  $\phi_{lm}$ , which guided the analysis towards 2D cuts on combinations of the  $\phi$  angles, which all had fairly good separation. Separation between  $\phi_{hm}$  and  $\phi_{lm}$  did prove to have the best separation of the  $\phi$  2D distributions, and was selected as a candidate for implementing 2D cuts. The 2D distributions for both  $\phi_{lh}vs.p^T$  and  $phi_{lm}vs.\phi_{hm}$  can be seen in Fig. 17.

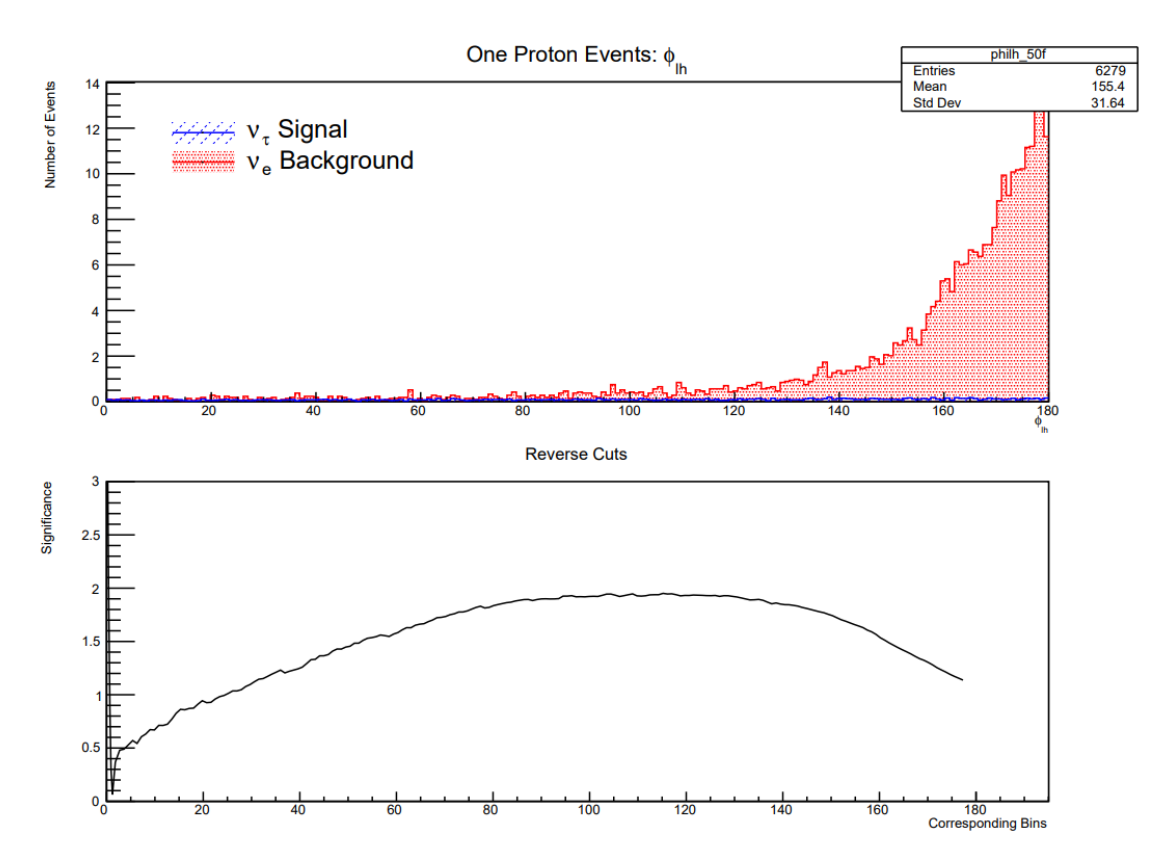


Figure 15: POT normalized  $\phi_{lh}$  with corresponding significance plot - peak at  $\sim 120$ 

The  $\phi_{lm}$  vs.  $\phi_{hm}$  plot has a distinct diagonal line of background events across the center, suggesting a linear cut shifted to the right of the background clumping. The final line chosen for the cut was  $y = 205 - 0.98 \cdot \phi_{hm}$ , which is roughly indicated by the purple line in Fig. 17b. This resulted in a background reduction of 299 events to 78 events ( $\sim 84\%$  cut), and a reduction in signal events from 18 events to 14 events (only  $\sim 22\%$  cut), giving a significance of  $\sim 1.6\sigma$ .

In the  $\phi_{lh}vs.p^T$  plot, there is a clear clumping of background events at low  $p^T$  and high  $\phi_{lh}$  which is precisely what is expected for  $\nu_e$ CC interactions (see Fig. 9). This gives the opportunity for an effective background cut on these two variables. The final optimized 2D selection cut out all events which had both  $p^T < 0.45$ GeV and  $\phi_{lh} > 120^\circ$  (see the purple region in Fig. 17a. After POT normalization and with event selection of only events with at least one electron and at least one proton with kinetic energy over 50 MeV, having no other final state charged particles, we are left with 18  $\nu_{\tau}$ CC events and 299  $\nu_e$ CC events. After this selection, background is reduced from 299  $\rightarrow$  18 events, an efficiency of 94%. This is very good for background rejection, but 50% of the signal events are also cut, going from 18  $\rightarrow$  9  $\nu_{\tau}$ CC events. This combined cut gives a significance of 2.12 $\sigma$ , which is the highest achieved with a 2D cut in this analysis, but would not be enough to declare signal detection in a real experiment.

# 4 Reconstruction Analysis

Following MC-truth level analysis, reconstruction analysis must be carried out based on the same simulated events. The first step of successful reconstruction analysis is to correctly identify the particle tracks and showers seen by MicroBooNE. Each charged particle detected by the LArTPC leaves a track or shower indicative of the type of particle it is. The first step of a successful reconstruction

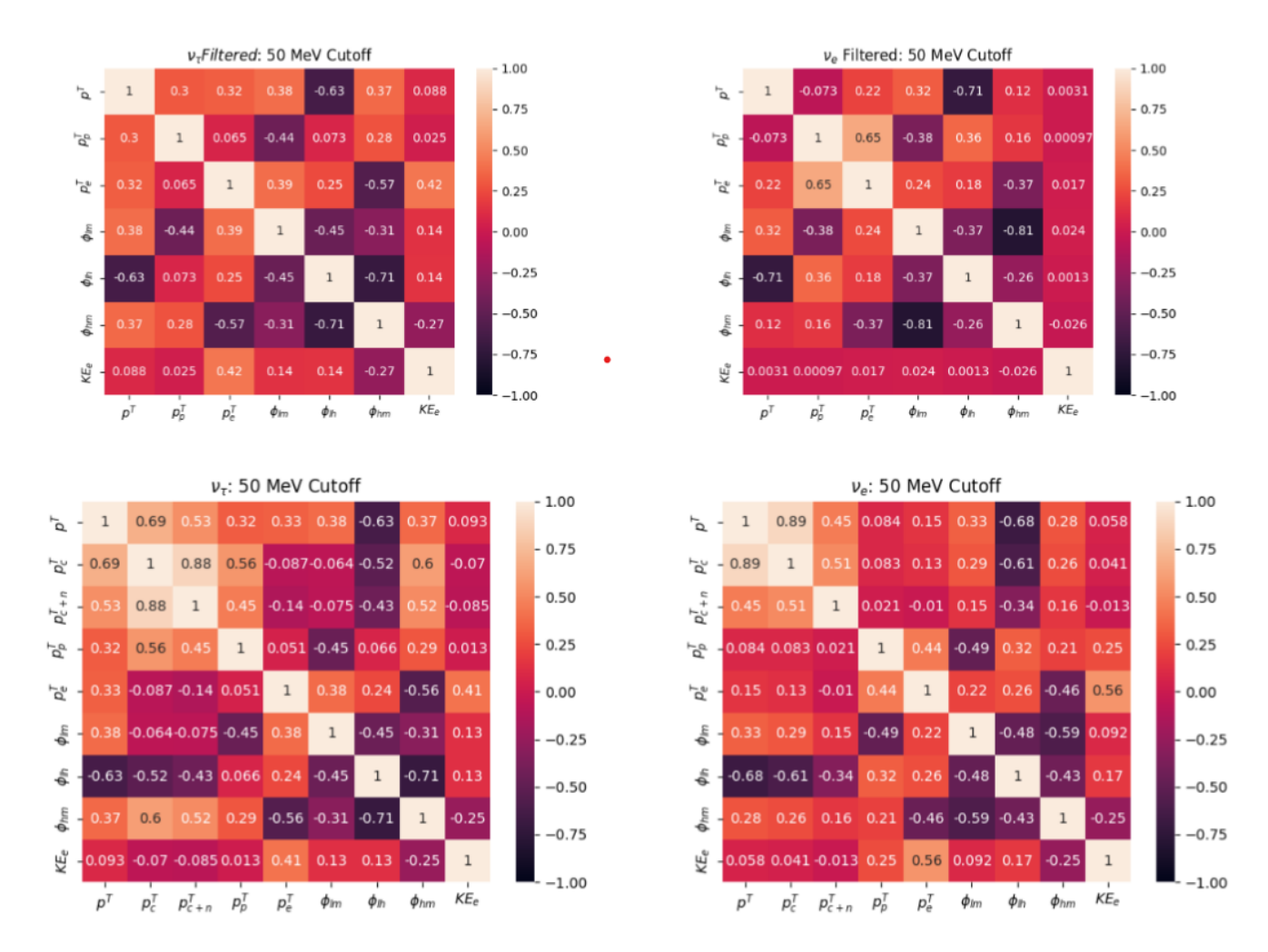


Figure 16: Kinematic variable correlation matrices for two pre-selection schemes, see both signal correlations on the left and background on the right.

analysis is to have an efficient selection for particle identification based on the reconstruction information given by GENIE and Pandora. We are mainly concerned with identifying proton and electron tracks, and don't particularly care to be able to correctly identify any of the other particles such as muons or pions that are common within these interactions. To develop a selection for proton-like tracks, events with only outgoing protons and muons in MC-truth were chosen and used to find the determining characteristics of a proton-like track. Events with no showers were selected in order to eliminate events with unwanted particles such as  $\Pi^0$ s. Within these events, it was required for there to be at least one long (> 1 meter) muon-like event, and one or more short (< 50 cm) proton-like events. A revision on the selection also allowed 50 cm - 100 cm tracks to be classified as muons for an energy deposition dE/dx less than 2, indicative of a minimum-ionizing particle. The efficiency of this selection is 81% for identifying at least one proton and one muon.

After this, the same idea was applied to  $\nu_{\tau}$ CC events with only protons and an electron in MC-truth, with the only cut applied to the showers being a 100 MeV minimum energy threshold. This resulted in a selection efficiency of 53% (1806 out of 3391 events had identified at least one proton and electron). While this is a decent number of events considering the only two variables taken into account are the length and whether the track indicates a high-ionizing particle (hip) or minimum-ionizing particle, and it can be used for preliminary reconstruction analysis, we really want a much better particle identification selection. There are many variables that can be used to determine

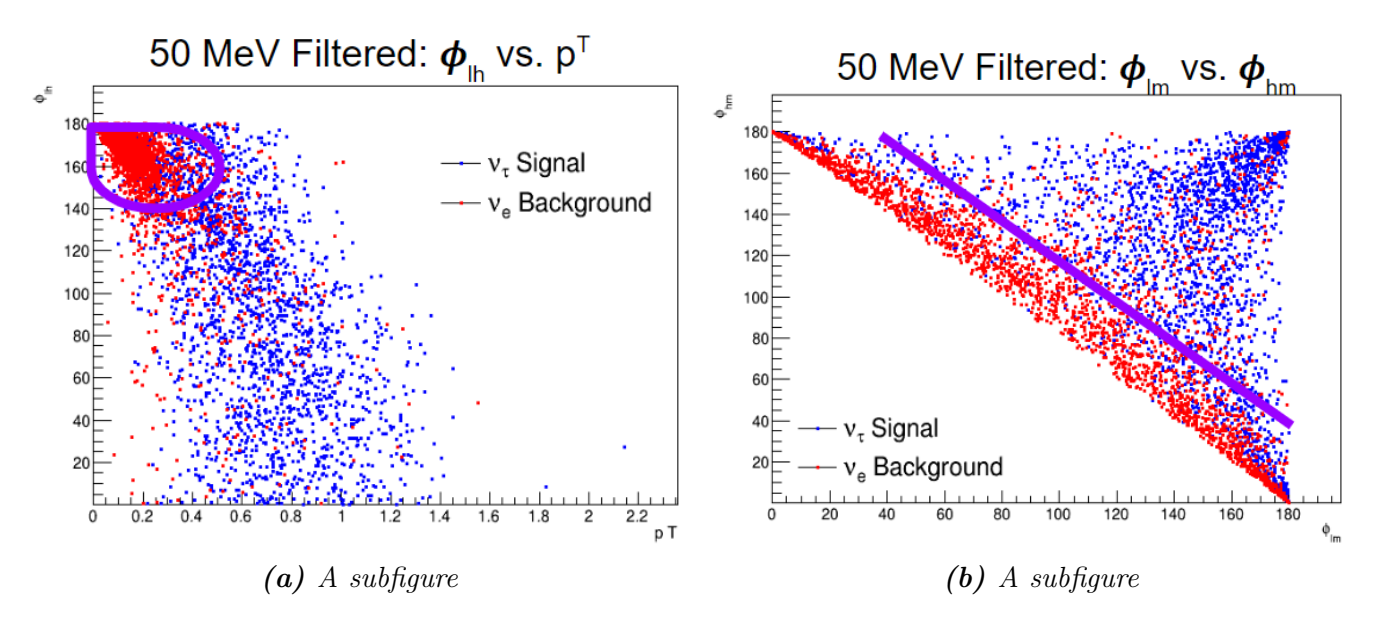


Figure 17: A figure with two subfigures

particle identification, but to make use of them all would require the development and training of a boosted decision tree (BDT) for track selection.

# 5 Conclusion & Next Steps

This project has resulted in developed tools to optimize selection for  $\nu_{\mu} \to \nu_{\tau}$  oscillation in MicroBooNE. The most effective background reducing event selection takes into account only events with an electron and at least one proton with a kinetic energy over 50 MeV. By taking out events that have extra charged particles, the number of background events is reduced from 19280 to 6279 (32%), while signal events only reduced from 3363 to 2332 (69%). Using the events which pass this event selection, further cuts were applied on the studied kinematic variables. The 1D selection with the highest signal to background statistical significance was on  $p^T$ , cutting all events with  $p^T$  less than 0.45 GeV. After applying this cut, we are left with 7 signal events and 10 background events, giving a significance of  $\sim 2.2\sigma$ .

In MicroBooNE, the energy region over 3.5 GeV already has low flux comparative to the peak energies under 1 GeV, and in combination with the restriction to the  $\tau \to e^- \bar{\nu}_e \nu_\tau$  branch of the tau decay, we are left with very low statistics for possible observable  $\nu_\tau$ CC events, even with 100% oscillation. Applying the optimal event selection of events with only an outgoing electron and protons (with 50 meV KE cutoff), and no other charged particles, the number of POT normalized signal events is reduced to just 18 (more inclusive event selections can get this number to 24, such as including events which DO have extra final state charged particles). Accounting for a more realistic oscillation probability of 10%, we are then looking for an excess of 1-2 signal events over the entire MicroBooNE run, which unfortunately cannot provide significance for any declaration of detection.

Although the chances of seeing a statistically significant number of  $\nu_{\tau}$  events in MicroBooNE seems unlikely, the continuation of this analysis would be valuable for the future SBN, with higher statistics from SBND and ICARUS. The new Short Baseline Near Detector (SBND) in particular is expected to enhance sensitivity by constraining neutrino flux and interaction uncertainties. Similar studies are also being done for DUNE, which will have the highest statistics for neutrino interactions thus far.

The most immediate next step would involve the development and training of a BDT using the xgBoost package for reconstruction particle identification. Efficient reconstructed particle identification would then allow testing for a new background rejection algorithm based on the reconstruction data. Once this is fully developed, it would be applied to the greater MicroBooNE Monte Carlo simulation, giving a theorized sensitivity to  $\nu_{\mu} \rightarrow \nu_{\tau}$  oscillaiton in MicroBooNE. Applying the same cuts to the SBND and ICARUS simulations would then give the first sensitivity calculation of  $\nu_{\mu} \rightarrow \nu_{\tau}$  for the full SBN program.

# 6 Acknowledgements

I would like to thank Dr. Georgia Karagiorgi, Dr. Michael Shaevitz, Dr. Leslie Camilleri, PhD candidate Guanqun Ge, and undergraduate student Eva Savin for their guidance and support. This material is based upon work supported by the National Science Foundation under Grant No. PHY/1950431.

## References

- [1] R. et al. Acciarri. A proposal for a three detector short-baseline neutrino oscillation program in the fermilab booster neutrino beam. 03 2015.
- [2] A. A. et al. Aguilar-Arevalo. Unexplained excess of electronlike events from a 1-gev neutrino beam. *Phys. Rev. Lett.*, 102:101802, Mar 2009.
- [3] Janet M. Conrad, William C. Louis, and Michael H. Shaevitz. The LSND and MiniBooNE oscillation searches at high {upDeltaim/isup2/sup. Annual Review of Nuclear and Particle Science, 63(1):45–67, oct 2013.
- [4] P. Abratenko et al. First constraints on light sterile neutrino oscillations from combined appearance and disappearance searches with the MicroBooNE detector. *Physical Review Letters*, 130(1), jan 2023.
- [5] R. Acciarri et al. Design and construction of the microboone detector. *Journal of Instrumentation*, 12(02):P02017, feb 2017.
- [6] Krishanu Majumdar and Konstantinos Mavrokoridis. Review of liquid argon detector technologies in the neutrino sector. *Applied Sciences*, 11:2455, 03 2021.
- [7] Fermilab Creative Services. Short baseline neutrino program at fermilab, June 2019.
- [8] M.and Particle Data Group et al. Tanabashi. Review of Particle Physics\*., 98(3):030001, August 2018.

# 7 Appendix

All of the code developed for this project are C++ scripts run in root, and can be found on GitHub at: https://github.com/GuanqunGe/Nu-Tau-Oscillation/tree/svick.

Decay Mode	Resonance	Branching Ratio (%)
Leptonic Decays		35.2
$\tau^- \to e^- \bar{\nu_e} \nu_{\tau}$		17.8
$\tau^- \to \mu^- \bar{\nu_\mu} \nu_\tau$		17.4
Hadronic Decays		64.8
$\tau^- \to h^- \nu_{\tau}$		11.5
$ au^-  o h^- \pi^0  u_ au$	$\rho(770)$	25.9
$ au^-  o h^- \pi^0 \pi^0 \nu_ au$	$a_1(1260)$	9.5
$ au^-  ightarrow h^- h^+ h^-  u_ au$	$a_1(1260)$	9.8
$\tau^- \to h^- h^+ h^- \pi^0 \nu_\tau$		4.8
Other		3.3

Table 1: Caption

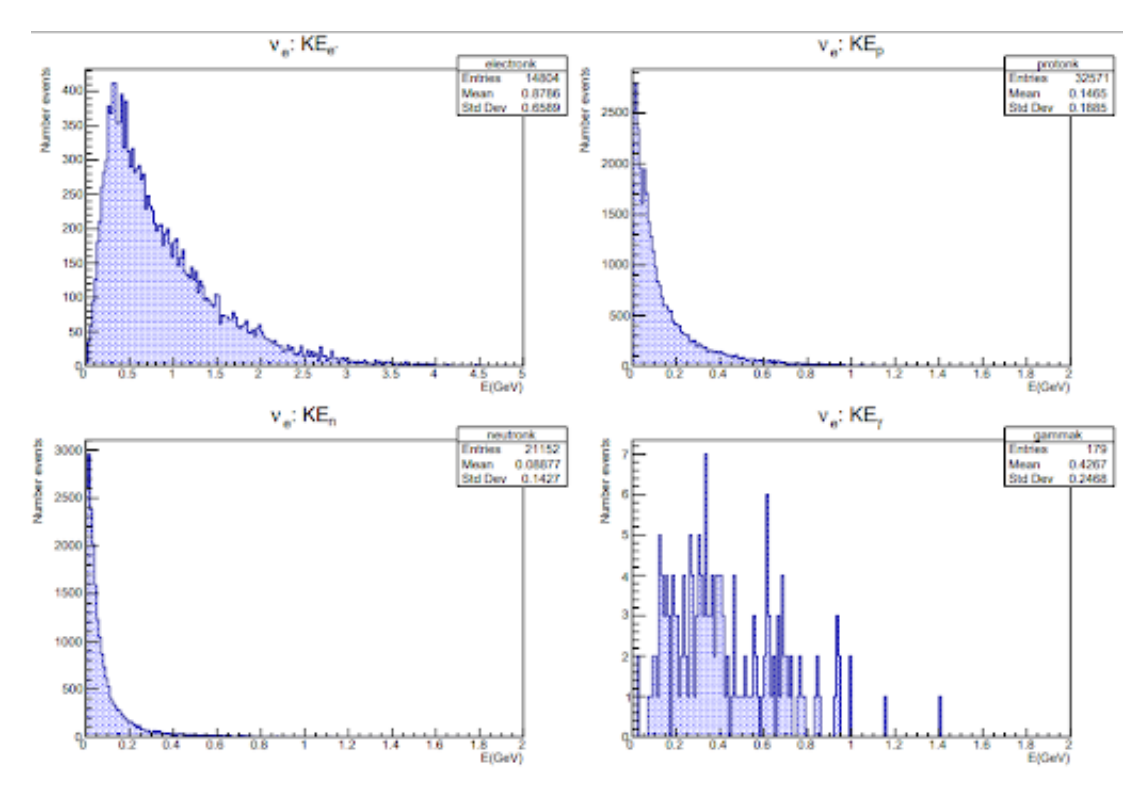


Figure 18:  $\nu_e$  kinetic energy of final state neutrons, protons, electrons and gammas.

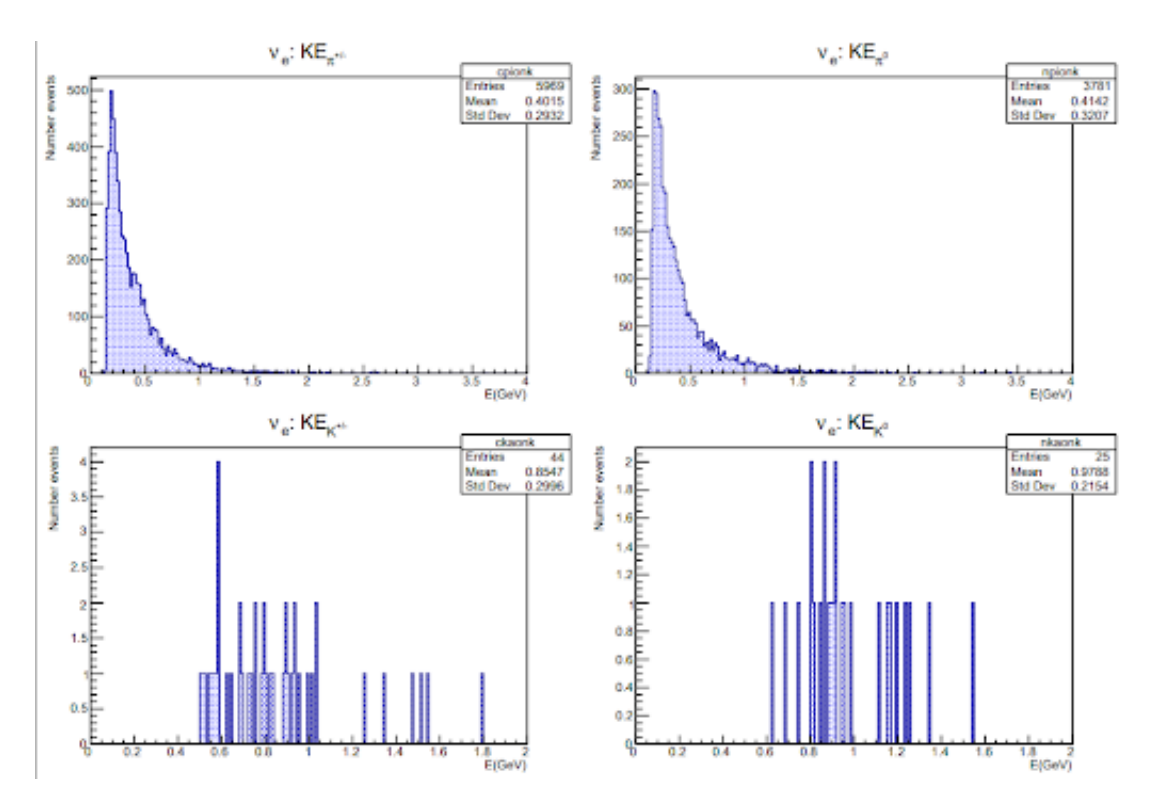


Figure 19:  $\nu_e$  kinetic energy of final state pions and kaons.

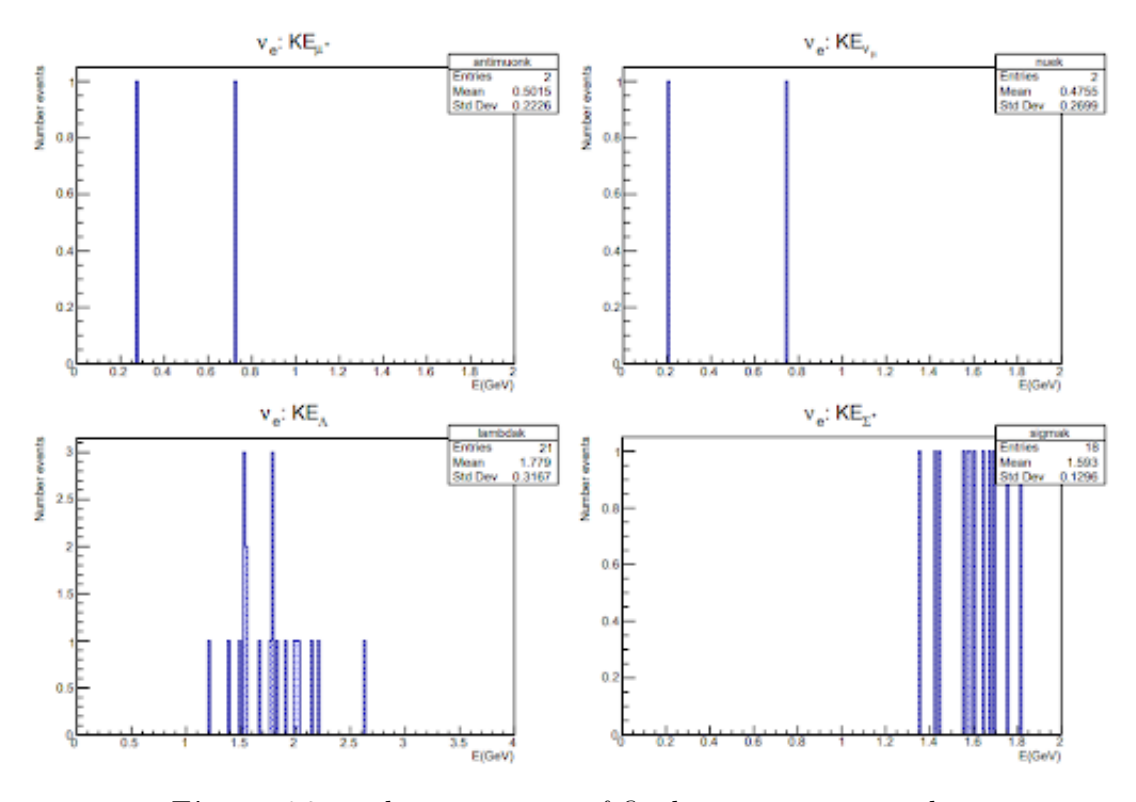


Figure 20:  $\nu_e$  kinetic energy of final state misc. particles.

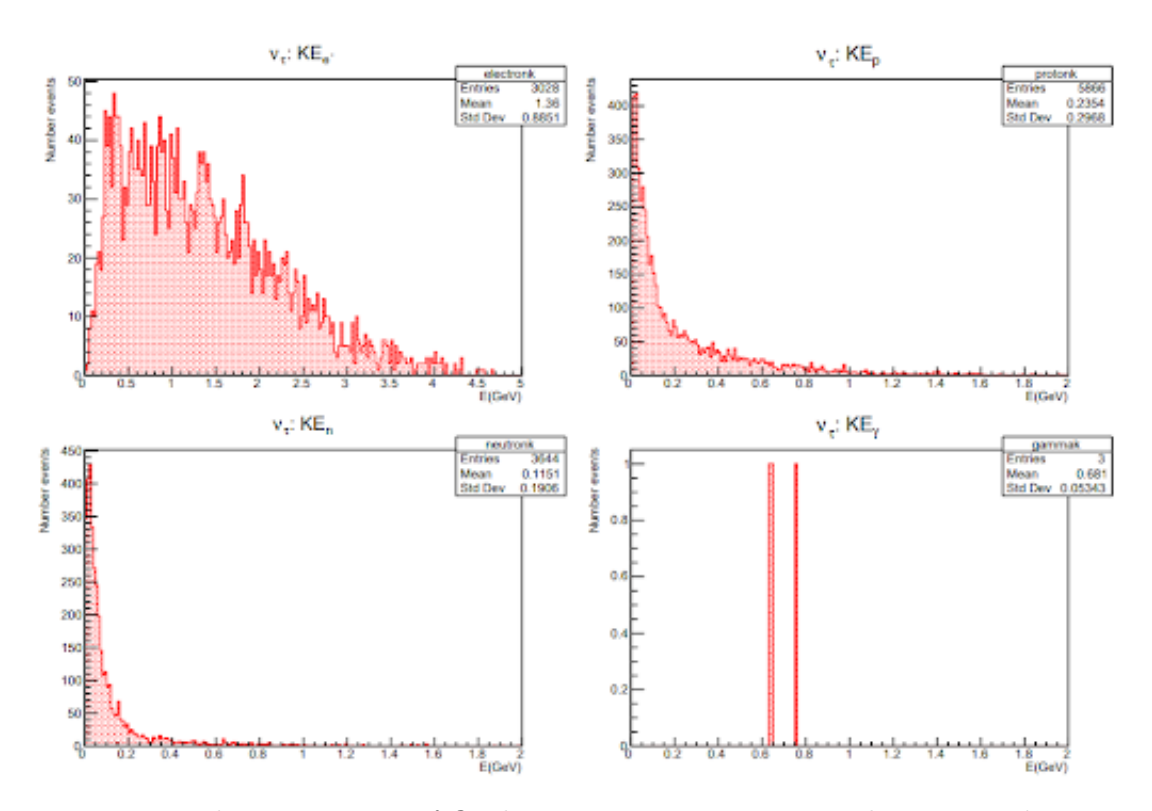


Figure 21:  $\nu_{\tau}$  kinetic energy of final state neutrons, protons, electrons and gammas.

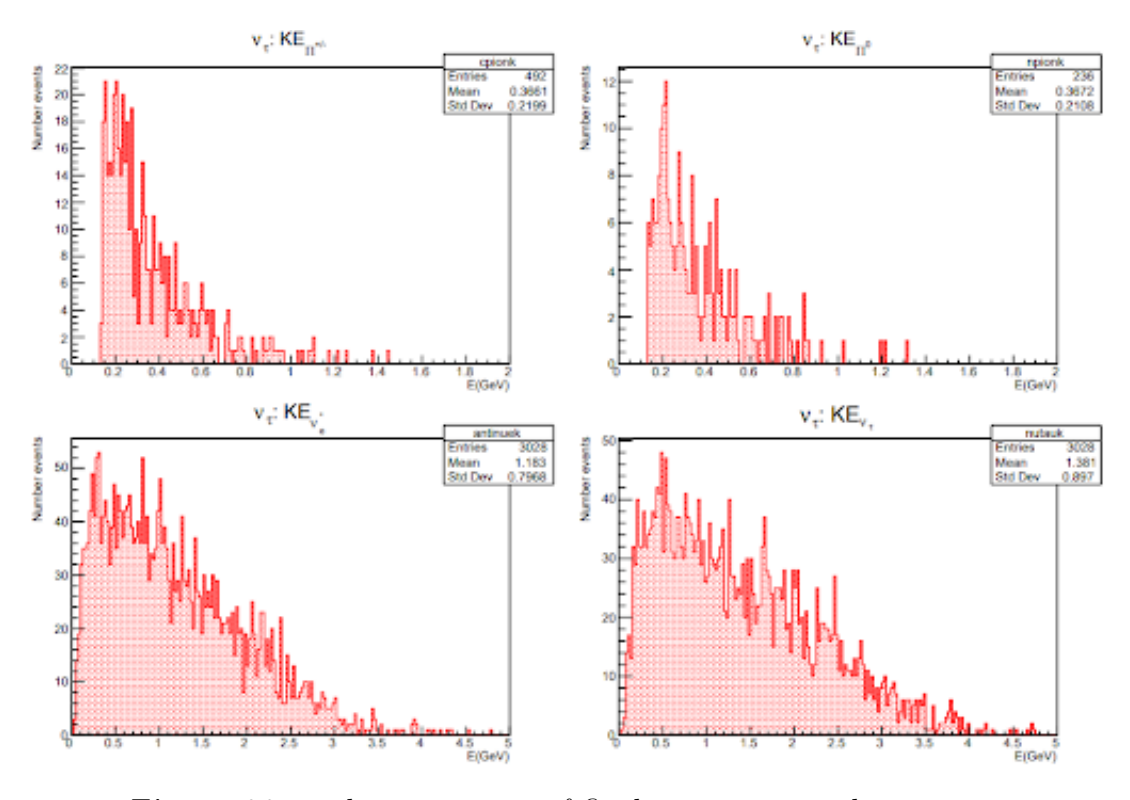


Figure 22:  $\nu_{\tau}$  kinetic energy of final state pions and neutrinos.